Dynamic resource allocation for virtualized wireless networks in massive-MIMO-aided and Front-haul-Limited C-RAN

Dynamic Resource Allocation for Virtualized Wireless Networks in Massive-MIMO-aided and Fronthaul-limited C-RAN

Saeedeh Parsaeefard*, Rajesh Dawadi†, Mahsa Derakhshani‡, Tho Le-Ngoc†, Mina Baghani*
* Communication Technologies & Department, ITRC, Tehran, Iran
†Department of Electrical & Computer Engineering, McGill University, Montreal, QC, Canada
‡Wolfson School of Mechanical, Electrical & Manufacturing Engineering, Loughborough University, UK
Email: s.parsaeifard@itrc.ac.ir; rajesh.dawadi@mail.mcgill.ca; m.derakhshani@lboro.ac.uk;
tho.le-ngoc@mcgill.ca; Baghani@aut.ac.ir

***Abstract*—This work considers the uplink dynamic resource allocation in a cloud radio access network (C-RAN) serving users belonging to different service providers (called slices) to form virtualized wireless networks (VWN). In particular, the C-RAN supports a pool of base-station (BS) baseband units (BBUs), which are connected to BS radio remote heads (RRHs) equipped with massive MIMO, via fronthaul links with limited capacity. Assuming that each user can be assigned to a single RRH-BBU pair, we formulate a resource allocation problem aiming to maximize the total system rate, constrained on the minimum rates required by the slices and the maximum number of antennas and power allocated to each user. The effects of pilot contamination error on the VWN performance are investigated and pilot duration is considered as a new optimization variable in resource allocation. This problem is inherently non-convex, NP-hard and thus computationally inefficient. By applying the successive convex approximation (SCA) and complementary geometric programming (CGP) approach, we propose a two-step iterative algorithm: one to adjust the RRH, BBU, and fronthaul parameters, and the other for power and antenna allocation to users. Simulation results illustrate the performance of the developed algorithm for VWNs in a massive-MIMO-aided and fronthaul-limited C-RAN, and demonstrate the effects of imperfect CSI estimation due to pilot contamination error, and the optimal pilot duration.**

***Index Terms*—Cloud-RAN, Complementary Geometric Programming, 5G, virtualized wireless networks, massive MIMO.**

I. Introduction

Virtualized wireless networks (VWN), cloud radio access network (C-RAN) and massive MIMO are the three key technologies envisioned for the fifth generation of wireless networks (5G) [1], [2], [3]. While they can considerably improve the resource utilization as well as increase the spectrum and energy efficiency of 5G, each of them suffers from their own implementation issues.

In a VWN, the resources, e.g., power, sub-carrier and antenna, are sliced to the multiple service providers (SPs) in order to increase the network utilization and reducing the CAPEX and OPEX [4]. Although VWNs can enhance spectral efficiency in wireless networks, to ensure the performance of each slice, the quality of service of users in one slice should not be affected by activity of users of other slices. This is refereed to as slice isolation. To maintain good isolation among slices while increasing network spectral efficiency, dynamic resource allocation needs to consider not only user-QoS requirements but also minimum throughput or resource for each slice, e.g., [4], [5].

In C-RAN, the base-station (BS) signal processing functionalities are moved into a pool of BBUs that are connected to the RRHs through a high-speed fronthaul link [6], aiming to reduce operational expenditure and to enhance spectrum efficiency. However, in C-RAN, the limited capacity of the fronthaul links poses a severe constraint on the maximum number of served users over the coverage of interest [7], [8]. Besides, the optimal utilization of the BBU processing resources to control the network overload is important to reach the best performance design [9].

With the recently proposed massive MIMO technique, the BS transceivers of wireless networks are equipped with a large number of antennas to provide spatial diversity gain. To fully exploit the gain from massive MIMO and minimize the interference among different transceivers in a multi-cell scenario, the perfect user-channel state information (CSI) is required. However, due to the pilot contamination error, the estimated values of CSI are subject to uncertainty, leading to the existence of interference [10].

In this work, considering the above limitations, we study the uplink dynamic resource allocation in a C-RAN serving users belonging to different service providers (or equivalently, slices) to enable wireless virtaulziation. The C-RAN covers a multi-cell area with a pool of BBUs connected to the RRHs, equipped with massive MIMO, through limited-capacity fronthaul links. Specifically, we consider the effects of C-RAN fronthaul capacity limitation and imperfect CSI due to pilot contamination in a multi-cell massive MIMO environment. To provide the isolation among slices, we consider minimum guaranteed rate and number of antennas for each slice. The limitation of C-RAN includes maximum transmit power, limited number of antennas of each RRH, finite fronthaul capacity, and maximum load of each BBU. With the objective to maximize the network sum-rate subject to the slice isolation and C-RAN constraints, we formulate the resource allocation problem that involves joint allocation of BBU, RRH, fronthaul,

Manuscript received March 19, 2017; and accepted May 22, 2017. This work was supported in part by a Natural Sciences and Engineering Research Council of Canada (NSERC) Collaborative RD Grant with Huawei Technologies Canada, and by Project 907950200 in ITRC. The review of this paper was coordinated by Dr. Dania Marabissi. Corresponding author is S. Parsaeefard (e-mail:s.parsaeifard@itrc.ac.ir and saeede.parsaeefard@gmail.com).

power, and antenna parameters.

The formulated optimization problem is inherently non-convex and NP-hard due to the inherent nature of wireless channels [11], intertwined sets of optimization variables, and a variety of constraints in this setup. To develop an efficient algorithm to solve the problem, we propose a two-step iterative algorithm with the aim to decompose the cloud and transmission parameters. The first step determines the cloud parameters for joint BBU, fronthaul and RRH allocation, while the second step derives the transmission parameters, including the transmit power and the number of allocated antennas to each user under the slice-based constraints. The problem for each step is still non-convex and NP-hard. We apply the complementary geometric programming (CGP) and successive approximation approach (SCA) via different relaxation and transformation techniques, the sub-problems in each step are transformed into the geometric programming (GP) counterparts [12], [13], which can be solved efficiently by optimization packages like CVX [14].

This work is in the intersection of two important classes of research in resource allocation problems: 1) resource allocation in C-RAN, 2) resource allocation in VWNs. Due to the importance of C-RAN in the architecture of 5G networks, there is a surge of research to study how to utilize the C-RAN resources in the optimal manner [3]. C-RAN facilitates the centralized resource allocation, however, due to the interference in the wireless networks, the resource allocation problems are more complex and non-convex, especially due to the new set of cloud-structure variables, e.g., front-haul assignment parameters. Consequently, proposing an efficient algorithm to solve this type of problems and tackling their related computational complexity are of high importance. For instance, in [15], the resources (power and antennas) in C-RAN are allocated to maximize the average weighted sum rate, which is solved via the weighted minimum mean square error method. Also, in [16], with the objective of increasing energy efficiency, the user association and beamforming parameters are adjusted in C-RAN where the norm approximation is used for transferring the non-convex problem to the convex one. In this paper, we apply CGP along with various transformations and convexification approaches to convert the problem to a convex one.

In parallel, by proposing the VWN, new challenges, e.g., isolation between slices, in resource allocation are addressed in the recent literatures [4]. For instance, the resource allocation problem in view of economic and cost perspectives is considered in [17], [18], [19], [20]. In [21], the average coverage probability and average throughput improvement are studied by a stochastic geometry approach. The network latency is minimized by user association in [22]. Also, in [23] joint power, subcarrier and antennas allocation is investigated with the aim of maximizing the energy efficiency. However, to the best of our knowledge, C-RAN and its practical benefits to increase isolation in a VWN are not studied in this literature.

Compared to two aforementioned classes of research, in this paper, the rate optimization problem is presented in virtualized C-RAN equipped with massive MIMO by considering both perfect and imperfect CSIs. We formulate the resource allocation in C-RAN based on the fronthaul and BBUs limitations. The imperfect channel estimation error happens due to pilot contamination between RRHs. More specifically, we consider time duration of pilot to estimate CSI as a new optimization variable. Then we demonstrate the trade-off between increasing CSI estimation accuracy and VWN throughput by increasing the pilot duration. To our best knowledge, in this context, such effect has not been explored. Accordingly, the optimal pilot duration is derived by simulation. In addition, we show that how by categorizing the variables of optimization problems in C-RAN, the effective iterative algorithm in two steps can be developed. Applying this approach, the complex multi-dimensional resource allocation is solved by the proposed algorithm with polynomial complexity.

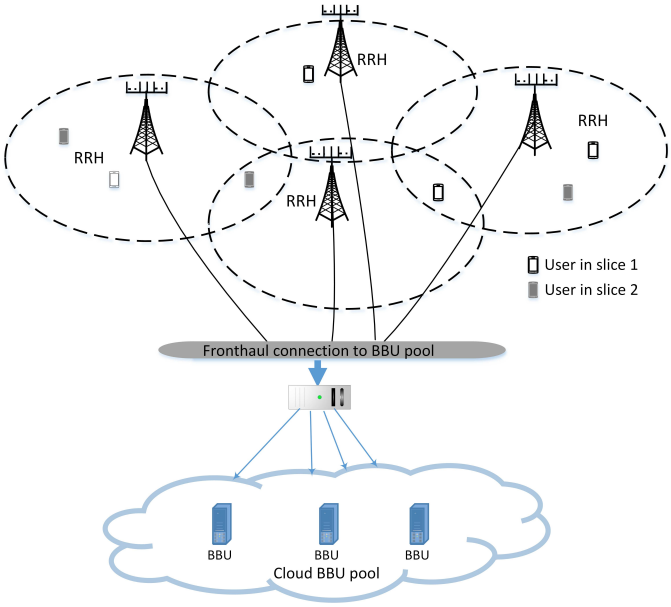

Fig. 1: Massive MIMO VWN's with C-RAN

The rest of this paper is organized as follows. Section II presents the system model and problem formulation. In Section III, the proposed algorithm is derived, followed by the simulation results in Section IV. Finally, Section V presents concluding remarks.

II. System Model

Consider the uplink transmission in a C-RAN supporting a set of $\mathcal{S} = \{1, \cdots, S\}$ slices (service providers). Each slice $s \in \mathcal{S}$ has a set of $\mathcal{K}_s = \{1, \cdots, K_s\}$ single-antenna users and requires a minimum rate R_s^{rsv} to support the QoS of its users. The C-RAN covers all the users by a set of $\mathcal{L} = \{1, \cdots, L\}$ RRHs and each RRH is equipped with $M \gg 1$ antennas (i.e., massive MIMO). Via a limited-capacity fronthaul link, each RRH is connected to a set of $\mathcal{B} = \{1, \cdots B\}$ BBUs to process the baseband signals. The system model of VWN with C-RAN architecture is illustrated in Fig. 1, where users belonging to different slices are served by multiple RRHs that are connected to the cloud of BBUs via the fronthaul link.

The association between the BBU b and the user k_s is represented by

$$f_{k_s,b} = \begin{cases} 1, & \text{if user } k_s \text{ in slice } s \text{ is supported by BBU } b, \\ 0, & \text{otherwise.} \end{cases}$$

Each BBU b can support at most $o_b^{\max}$ users [24], i.e.,

$$\text{C1: } \sum\nolimits_{s\in\mathcal{S}}\sum\nolimits_{k_s\in\mathcal{K}_s} w_{k_s,b} f_{k_s,b} \le o_b^{\max}, \quad \forall b\in\mathcal{B},$$

where $w_{k_s,b}$ is the load balancing factor for the BBU b to the user k_s, which is a system parameter and is a random number assigned by the VWN to control the traffic and load of each BBU-user pair. We define F_{k_s} for each user k_s as

$$\text{C2: } F_{k_s} = \sum\nolimits_{b\in\mathcal{B}} f_{k_s,b}, \quad \forall k_s\in\mathcal{K}_s, \forall s\in\mathcal{S}.$$

Define α_{l,k_s} as the user association factor (UAF) indicating the association between RRH l and user k_s, i.e.,

$$\alpha_{l,k_s} = \begin{cases} 1, & \text{if user } k_s \text{ in slice } s \text{ is connected to RRH } l, \\ 0, & \text{otherwise,} \end{cases}$$

We assume that each user can be only connected to at most one RRH at a time, i.e.,

$$\text{C3: } \sum\nolimits_{l\in\mathcal{L}} \alpha_{l,k_s} \le 1, \quad \forall k_s\in\mathcal{K}_s, \forall s\in\mathcal{S}. \tag{1}$$

To further control the C-RAN load, we assume that each user is supported by only one BBU at each transmission instance, if and only if, it is assigned to at least one RRH, i.e.,

$$\text{C4: } F_{k_s} = \sum\nolimits_{\forall l\in\mathcal{L}} \alpha_{l,k_s}, \ \forall k_s\in\mathcal{K}_s, \ \forall s\in\mathcal{S}.$$

C2 and C4 together make sure that F_{k_s} , the total number of BBUs supporting user k_s, must equal the total number of RRHs connected to user k_s, so that the C-RAN BBU resources are not wasted. F_{k_s} is also used as an auxiliary variable that helps to convert non-convex optimization problems of this paper to the GP-based ones. Consider that the fronthaul link between RRH l and BBU b has a capacity of $c_{l,b}^{\max}$ [25]. Then, we also have the following practical constraint

$$\text{C5: } \sum\nolimits_{s\in\mathcal{S}}\sum\nolimits_{k_s\in\mathcal{K}_s} f_{k_s,b}\alpha_{l,k_s} \le c_{l,b}^{\max}, \quad \forall b\in\mathcal{B}, \ \forall l\in\mathcal{L}.$$

Denote $h_{l,k_s,m}$ as the channel coefficient from user k_s to antenna m of RRH l and $\mathbf{h}_{l,k_s}\in\mathbb{C}^{1\times M_{l,k_s}}$ as the uplink channel vector of user k_s where M_{l,k_s} is the total allocated antennas by RRH l to user k_s. More specifically, $h_{l,k_s,m}$ is [26]

$$h_{l,k_s,m} = \chi_{l,k_s,m}\sqrt{\beta_{l,k_s}}$$

where $\chi_{l,k_s,m}$ represents the small-scale multipath fading coefficient from user k_s to the antenna m of RRH $l\in\mathcal{L}$ and β_{l,k_s} denotes the large-scale power loss due to path loss and shadowing from user k_s to RRH $l\in\mathcal{L}$ [26]. Since the distance between the antennas in a RRH can be assumed to be negligible compared to the distance between the RRH l and user k_s, β_{l,k_s} is independent over the antennas, m [27]. Practically, the CSIs are estimated by the RRHs based on the up-link pilots with duration τ at the specific part of the coherence interval of T. If the orthogonality of pilot signals in the multi-cell scenario of massive MIMO based networks can be preserved,CSI estimation would be perfect and the SINR of user k_s in slice s at RRH l becomes (See Appendix A-1 and [27])

$$\gamma_{l,k_s}^{\text{Perfect}} = \beta_{l,k_s}P_{l,k_s}M_{l,k_s}, \quad \forall k_s\in\mathcal{K}_s, \forall s\in\mathcal{S}, \tag{2}$$

Algorithm 1 Iterative Joint User Association and Resource Allocation Algorithm

Initialization: Set $t := 1$ and initialize all power of each user by $P_{k_s}^{\max}$, and all antennas by $[M_l^{\max}/K]$.
Repeat
Step 1: Derive $\boldsymbol{\alpha}^*(t)$ and $\mathbf{F}^*(t)$ from (7) by considering fixed values of $\mathbf{P}^*(t-1)$ and $\mathbf{M}^*(t-1)$;
Step 2: For fixed values of $\boldsymbol{\alpha}^*(t)$ and $\mathbf{F}^*(t)$, find $\mathbf{P}^*(t)$ and $\mathbf{M}^*(t)$ from (14) or (18);
Step 3: Stop if $||\mathbf{P}^*(t)-\mathbf{P}^*(t-1)||\le\varepsilon_1$, and $||\mathbf{M}^*(t)-\mathbf{M}^*(t-1)||\le\varepsilon_2$. Otherwise, set $t := t+1$ and go to **Step 1**.

where P_{l,k_s} is the transmit power of user k_s to RRH l and the noise for all users and RRHs is normalized to 1. On the other hand, considering the pilot contamination error, there is *Imperfect CSI* estimation and the SINR of user k_s in slice s to RRH $l\in\mathcal{L}$ becomes (See Appendix A-2 and [27])

$$\gamma_{l,k_s}^{\text{Imperfect}} = \frac{\tau\beta_{l,k_s}^2 P_{l,k_s}^2 M_{l,k_s}}{\tau\sum\limits_{\forall s\in\mathcal{S}}\sum\limits_{\forall l'\in\mathcal{L}}\sum\limits_{\forall k_s'\in\mathcal{K}_s}\beta_{l',k_s'}^2 P_{l',k_s'}^2 M_{l',k_s'} + 1}. \tag{3}$$

Consequently, the rate of each user k_s at the RRH l is

$$R_{l,k_s} = \begin{cases} \log_2(1+\gamma_{l,k_s}^{\text{Perfect}}), \ \text{perfect CSI,} \\ \frac{T-\tau}{T}\log_2(1+\gamma_{l,k_s}^{\text{Imperfect}}), \text{imperfect CSI,} \end{cases} \tag{4}$$

To provide the isolation among slices, both rate and resource reservation strategies will be considered. In other words, the minimum required rate, R_s^{rsv}, and the minimum number of antennas, M_s^{rsv}, for each slice s are preserved [28]. These two isolation constraints in the VWN can be written as

$$\text{C6: } \sum\nolimits_{\forall l\in\mathcal{L}}\sum\nolimits_{\forall k_s\in\mathcal{K}_s} F_{k_s}\alpha_{l,k_s}R_{l,k_s} \ge R_s^{\text{rsv}}, \quad \forall s\in\mathcal{S},$$
$$\text{C7: } \sum\nolimits_{\forall l\in\mathcal{L}}\sum\nolimits_{\forall k_s\in\mathcal{K}_s} M_{l,k_s} \ge M_s^{\text{rsv}}, \quad \forall s\in\mathcal{S}.$$

From the hardware limitation, each user's transmit power and the number of RRH's antennas are limited as

$$\text{C8: } P_{l,k_s} \le P_{k_s}^{\max}, \quad \forall k_s\in\mathcal{K}_s, \forall s\in\mathcal{S}, \forall l\in\mathcal{L},$$
$$\text{C9: } \sum\nolimits_{s\in\mathcal{S}}\sum\nolimits_{k_s\in\mathcal{K}_s} M_{l,k_s} \le M_l^{\max}, \quad \forall l\in\mathcal{L},$$

where $P_{k_s}^{\max}$ and $M_l^{\max}$ are the maximum transmit power of user k_s and maximum number of antennas mounted on the RRH l, respectively. We assume $\sum_{s\in\mathcal{S}} M_s^{\text{rsv}} \le M_l^{\max}$ to eliminate the redundancy between C7 and C9.

With the objective of maximizing the total throughput of VWN subject to all the above implementation constraints, the resource allocation problem of this setup can be written as

$$\max_{\boldsymbol{\alpha},\mathbf{F},\mathbf{P},\mathbf{M}} \sum\nolimits_{\forall s\in\mathcal{S}}\sum\nolimits_{\forall l\in\mathcal{L}}\sum\nolimits_{\forall k_s\in\mathcal{K}_s} F_{k_s}\alpha_{l,k_s}R_{l,k_s}(\mathbf{P},\mathbf{M}), \tag{5}$$

subject to: C1 - C9,

where $\boldsymbol{\alpha}$, $\mathbf{F}$, $\mathbf{P}$, and $\mathbf{M}$ are the vectors of all α_{l,k_s}, $f_{k_s,b}$, P_{l,k_s}, and M_{l,k_s}, respectively, for all $k_s\in\mathcal{K}_s$, $s\in\mathcal{S}$, and $l\in\mathcal{L}$. Considering F_{k_s} and α_{l,k_s} in the rate of C-RAN is necessary to reach the practical rate. (5) suffers from a high computational complexity due to its non-convex and combinatorial structure.

III. Proposed two-step Iterative Algorithm

In order to solve (5), we propose a two-step iterative algorithm. In each iteration t, Step 1 computes the best values for the UAF parameters ($\boldsymbol{\alpha}$) and BBU association factors ($\mathbf{F}$) based on the values for $\mathbf{P}$ and $\mathbf{M}$ obtained in the previous iteration $(t-1)$. Subsequently, based on these newly derived values $\boldsymbol{\alpha}^*(t)$ and $\mathbf{F}^*(t)$, Step 2 solves for the RRH parameters, $\mathbf{P}^*(t)$ and $\mathbf{M}^*(t)$. The whole process can be represented as

$$\underbrace{\boldsymbol{\alpha}(0), \mathbf{F}(0) \rightarrow \mathbf{P}(0), \mathbf{M}(0)}_{\text{Initialization}} \rightarrow \underbrace{\boldsymbol{\alpha}(t)^*, \mathbf{F}(t)^* \rightarrow \mathbf{P}(t)^*, \mathbf{M}(t)^*}_{\text{Iteration } t}$$
$$\cdots \rightarrow \underbrace{\boldsymbol{\alpha}^*, \mathbf{F}^* \rightarrow \mathbf{P}^*, \mathbf{M}^*}_{\text{Optimal solution}}.$$

For $0 < \varepsilon_1 \ll 1$ and $0 < \varepsilon_2 \ll 1$, the iterative procedure is stopped when

$$||\mathbf{P}^*(t) - \mathbf{P}^*(t-1)|| \leq \varepsilon_1, ||\mathbf{M}^*(t) - \mathbf{M}^*(t-1)|| \leq \varepsilon_2.$$

Note that both problems in each step for finding optimal values are still non-convex and suffer from high computational complexity. To solve them efficiently, by applying CGP [12] along with various transformations and convexification approaches, the sequence of lower bound geometric programming based approximation is derived. We refer interested reader about CGP to Appendix A in [13]. The sub-algorithms are described in details in the following subsections.

A. Association Algorithm

For the obtained $\mathbf{P}(t-1)$ and $\mathbf{M}(t-1)$, at iteration t, the resource allocation problem is simplified into

$$\max_{\boldsymbol{\alpha}, \mathbf{F}} \sum_{\forall s} \sum_{\forall l} \sum_{\forall k_s} F_{k_s}(t) \alpha_{l,k_s}(t) R_{l,k_s}(\mathbf{P}(t-1), \mathbf{M}(t-1)),$$
$$\text{subject to: C1} - \text{C6} \tag{6}$$

Note that (6) is less computationally complex than (5), but is still non-convex. To further reduce the computational complexity, we first relax α_{l,k_s} from an integer to a continuous variable as $\alpha_{l,k_s} \in [0,1]$. To convert the resulting problem, we consider t_1 as the index of iteration in Step 1.

Proposition 1: In each iteration, the GP based approximation of (6) is

$$\min_{\boldsymbol{\alpha}(t_1), \mathbf{F}(t_1), x_0(t_1)} x_0(t_1), \text{ subject to:} \tag{7}$$
$$x_1 \big[\frac{x_0(t_1)}{c_0(t_1)}\big]^{-c_0(t_1)} \prod_{\forall l,k_s} \big[\frac{F_{k_s}(t_1)\alpha_{l,k_s}(t_1)R_{l,k_s}(t)}{c_{l,k_s}(t_1)}\big]^{-c_{l,k_s}(t_1)} \leq 1$$
$$\text{C1: } \sum\nolimits_{\forall s \in \mathcal{S}} \sum\nolimits_{k_s = \mathcal{K}_s} f_{k_s,b}(t_1) \leq o_b^{\max}, \quad \forall b \in \mathcal{B},$$
$$\widetilde{\text{C2}} : F_{k_s}(t_1) \prod\nolimits_{b \in \mathcal{B}} \big[\frac{w_{k_s,b} f_{k_s,b}(t_1)}{d_{k_s,b}(t_1)}\big]^{-d_{k_s,b}(t_1)} = 1, \forall k_s, \forall s$$
$$\text{C3:} \sum\nolimits_{\forall l} \alpha_{l,k_s} \leq 1, \quad \forall k_s \in \mathcal{K}_s, \forall s \in \mathcal{S},$$
$$\widetilde{\text{C4}} : F_{k_s}(t_1) \frac{1}{z_{k_s}} \prod\nolimits_{\forall l} \left[\frac{\alpha_{l,k_s}(t_1)}{e_{l,k_s}(t_1)}\right]^{-e_{l,k_s}(t_1)} = 1, \forall k_s, \forall s,$$
$$\text{C5: } \sum\nolimits_{s \in \mathcal{S}} \sum\nolimits_{\forall k_s \in \mathcal{K}_s} f_{k_s,b}(t_1) \alpha_{l,k_s}(t_1) \leq c_{l,b}^{\max}, \quad \forall b \in \mathcal{B},$$
$$\widetilde{\text{C6}} : R_s^{\text{rsv}} \prod\nolimits_{\forall l,k_s} \big[\frac{F_{k_s}(t_1)\alpha_{l,k_s}(t_1)R_{l,k_s}(t)}{\varphi_{l,k_s}(t_1)}\big]^{-\varphi_{l,k_s}(t_1)} \leq 1, \forall s.$$

where $\kappa_{l,k_s}(t_1 - 1) = \sum_{s \in \mathcal{S}} \sum_{\forall l \in \mathcal{L}} \sum_{\forall k_s \in \mathcal{K}_s} F_{k_s}(t_1 - 1)\alpha_{l,k_s}(t_1 - 1)R_{l,k_s}(t)$ and

$$c_0(t_1) = x_0(t_1 - 1)/[x_0(t_1 - 1) + \kappa_{l,k_s}(t_1 - 1)], \tag{8}$$
$$c_{l,k_s}(t_1) = \frac{F_{k_s}(t_1 - 1)\alpha_{l,k_s}(t_1 - 1)R_{l,k_s}(t)}{x_0(t_1 - 1) + \kappa_{l,k_s}(t_1 - 1)}, \tag{9}$$
$$d_{k_s,b}(t_1) = \frac{w_{k_s,b} f_{k_s,b}(t_1 - 1)}{\sum_{\forall b \in \mathcal{B}} w_{k_s,b} f_{k_s,b}(t_1 - 1)}, \forall k_s, \forall s, \forall b, \tag{10}$$
$$\varphi_{l,k_s}(t_1) = \frac{F_{k_s}(t_1 - 1)\alpha_{l,k_s}(t_1 - 1)R_{l,k_s}(t)}{\sum_{\forall l} \sum_{\forall k_s} F_{k_s}(t_1 - 1)\alpha_{l,k_s}(t_1 - 1)R_{l,k_s}(t)}, \tag{11}$$
$$e_{l,k_s}(t_1) = \frac{\alpha_{l,k_s}(t_1 - 1)}{\sum_{\forall l \in \mathcal{L}} \alpha_{l,k_s}(t_1 - 1)}, \forall k_s, \forall s, \forall l. \tag{12}$$

Proof. See Appendix B. □

Consequently, (7) can be solved efficiently via CVX at each iteration t_1. The iterative algorithm is initiated with an arbitrary value for $x_0(t_1) > 0$. Then, at each iteration, the approximation weights given by (10) are derived, and $\boldsymbol{\alpha}(t_1)$ and $\mathbf{F}(t_1)$ are updated. The iterative algorithm will be stopped if $||\boldsymbol{\alpha}^*(t_1) - \boldsymbol{\alpha}^*(t_1 - 1)|| \leq \varepsilon_1$, and $||\mathbf{F}^*(t_1) - \mathbf{F}^*(t_1 - 1)|| \leq \varepsilon_2$ where $0 < \varepsilon_1 \ll 1$ and $0 < \varepsilon_2 \ll 1$.

B. RRH Adjusting Algorithms

For fixed value of $\boldsymbol{\alpha}$ and $\mathbf{F}$ obtained from step 1, the resource allocation problem is simplified into

$$\max_{\mathbf{P}, \mathbf{M}} \sum_{s \in \mathcal{S}} \sum_{\forall l \in \mathcal{L}} \sum_{\forall k_s \in \mathcal{K}_s} F_{k_s}(t) \alpha_{l,k_s}(t) R_{l,k_s}(\mathbf{P}, \mathbf{M}), \tag{13}$$
$$\text{subject to: C6} - \text{C9}.$$

Similar to (6), (13) is less computationally complex than (5) as it only involves $\mathbf{P}$ and $\mathbf{M}$. However, it is non-convex. To reduce the computational complexity, we first relax M_{l,k_s} from an integer to a continuous variable in $[0, M_l^{\max}]$, then we apply the CGP framework to convert (13) into its GP based approximation as shown in the Proposition 2, where t_2 is the index of iteration Step 2.

Proposition 2: GP approximation of (13) is

• *Perfect CSI*

$$\min_{\mathbf{P}, \mathbf{M}} \prod\nolimits_{l,k_s,s} \Big[\big(\omega_{l,k_s}(t_2)\big)^{\omega_{l,k_s}(t_2)} \times \big(\beta_{l,k_s} P_{l,k_s}(t_2) M_{l,k_s}(t_2)/j_{l,k_s}(t_2)\big)^{-j_{l,k_s}(t_2)}\Big], \tag{14}$$
$$\text{subject to: C8, C9,}$$
$$\overline{\text{C6}} : \prod\nolimits_{l,k_s} \Big[\big(\omega_{l,k_s}(t_2)\big)^{\omega_{l,k_s}(t_2)} \times \big(\beta_{l,k_s} P_{l,k_s}(t_2) M_{l,k_s}(t_2)/j_{l,k_s}(t_2)\big)^{-j_{l,k_s}(t_2)}\Big]^{F_{k_s}(t)} \leq 2^{-R_s^{\text{rsv}}}, \forall s.$$
$$\overline{\text{C7}} : M_s^{\text{rsv}} \prod\nolimits_{\forall l,k_s} \big[[M_{l,k_s}(t_2)]/[\lambda_{l,k_s}(t_2)]\big]^{-\lambda_{l,k_s}} \leq 1, \quad \forall s \in \mathcal{S}.$$

where

$$\omega_{l,k_s}(t_2) = [1 + \beta_{l,k_s} P_{l,k_s}(t_2 - 1) M_{l,k_s}(t_2 - 1)]^{-1} \tag{15}$$
$$j_{l,k_s}(t_2) = \frac{\beta_{l,k_s} P_{l,k_s}(t_2 - 1) M_{l,k_s}(t_2 - 1)}{1 + \beta_{l,k_s} P_{l,k_s}(t_2 - 1) M_{l,k_s}(t_2 - 1)} \tag{16}$$

$$\lambda_{l,k_s}(t_2) = M_{l,k_s}(t_2-1)/[\sum_{\forall ks\in\mathcal{K}_s}\sum_{l\in\mathcal{L}} M_{l,k_s}(t_2-1)]. \quad (17)$$

• *Imperfect CSI*

$$\min_{\mathbf{P},\,\mathbf{M}} \prod_{l,k_s,s}\Bigg[(1+\tau\sum_{\forall l'\neq l}\sum_{\forall k'_s\neq k_s}\sum_{\forall s\in\mathcal{S}}\beta^2_{l',k'_s}P^2_{l',k'_s}(t_2) \quad (18)$$
$$\times M_{l',k'_s}(t_2))\times g_1(t_2)^{g_1(t_2)}\times$$
$$\prod_{\forall l,k_s}\Big[\frac{\tau\beta^2_{l,k_s}P^2_{l,k_s}(t_2)M_{l,k_s}(t_2)}{g_{l,k_s}(t_2)}\Big]^{-g_{l,k_s}(t_2)}\Bigg]$$

subject to: $\overline{\text{C}}7$, C8, C9,

$$\hat{\text{C}}6: \prod_{\forall l,k_s}\Bigg[(1+\tau\sum_{\forall l'\neq l}\sum_{\forall k'_s\neq k_s}\beta^2_{l',k'_s}P^2_{l',k'_s}(t_2)$$
$$\times M_{l',k'_s}(t_2))\times g_1(t_2)^{g_1(t_2)}\times$$
$$\prod_{\forall l,k_s}\Big[\frac{\tau\beta^2_{l,k_s}P^2_{l,k_s}(t_2)M_{l,k_s}(t_2)}{g_{l,k_s}(t_2)}\Big]^{-g_{l,k_s}(t_2)}\Bigg]^{F_{k_s}(t)} \leq 2^{-R^{\text{rsv}}_s}, \forall s,$$

where, $\theta_{l,k_s}(t_2) = \tau\sum_{\forall l\in\mathcal{L}}\sum_{\forall k_s\in\mathcal{K}_s}\sum_{\forall s\in\mathcal{S}}\beta^2_{l,k_s}P^2_{l,k_s}(t_2-1)M_{l,k_s}(t_2-1)$, and,

$$g_1(t_2) = 1/[1+\theta_{l,k_s}(t_2)], \quad (19)$$
$$g_{l,k_s}(t_2) = \frac{\tau\beta^2_{l,k_s}P^2_{l,k_s}(t_2-1)M_{l,k_s}(t_2-1)}{1+\theta_{l,k_s}(t_2)}. \quad (20)$$

Proof. See Appendix C. □

At each iteration problem (14) or (18) can be solved via CVX. The iterative algorithm will be stopped if $||\mathbf{P}(t_2) - \mathbf{P}(t_2-1)|| \ll \varepsilon_3$ and $||\mathbf{M}(t_2) - \mathbf{M}(t_2-1)|| \ll \varepsilon_4$, where $0<\varepsilon_3\ll 1$ and $0<\varepsilon_4\ll 1$.

IV. Computational Complexity and Convergence

In this section, we analyze the computational complexity and convergence of Algorithm 1. Since CVX is used to solve GP sub-problems with the interior point method in Steps 1 and 2, the number of required iterations is $\frac{\log(c/(t^0\varrho))}{\log(\xi)}$ [29], where c is the total number of constraints, t^0 is the initial point to approximate the accuracy of interior point method, $0<\varrho\ll 1$ is the stopping criterion for interior point method, and ξ is used for updating the accuracy of interior point method [29]. The numbers of constraints in (7) are $c_1 = 2B+3K_sS+S+1$ for Step 1 and $c_2 = 2S+K_sS+L$ for Step 2.

Moreover, for each iteration, the number of computations required to convert the non-convex problems using arithmetic-geometric mean approximation (AGMA) into the GP approximations is $i_1 = SK_sL+2K_sS+B+2L+K_sL$ and $i_2 = 2K_sL+SK_s$, in Step 1 and 2, respectively. Therefore, the computational complexity is $i_1\times\frac{\log(c_1/(t^0_1\varrho_1))}{\log(\xi_1)}$ for Step 1 and $i_2\times\frac{\log(c_2/(t^0_2\varrho_2))}{\log(\xi_2)}$ for Step 2.

Since the proposed algorithm follows the block coordinate descent (BCD) method, its convergence is guaranteed [30]. In particular, at each BCD iteration, a single block of variables is optimized, while the remaining variables are held fixed. The BCD convergence is guaranteed when the subproblem solution in each iteration is its global optimum. In [30], the convergence of an alternative inexact BCD approach is proved for the case where the variable blocks are updated by successive sequence of approximations of the objective function, which are either locally tight upper-bounds or strictly convex local approximations of the objective function, similar to the proposed algorithm. Although by convex approximation of subproblems, the convergence of the proposed algorithm is guaranteed, the convergence to the global optimum is not.

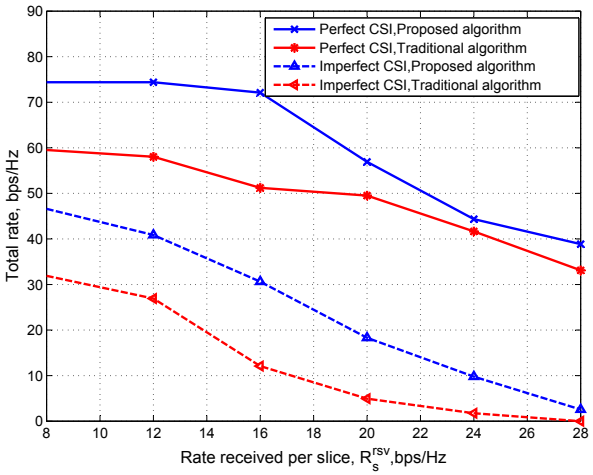

Fig. 2: Total rate versus R^{rsv}_s for $P^{\max}_{k_s} = 0$ dB, $M^{\max}_l = 150$, $L=4$, $B=3$, $o^{\max}_b = 8$, $K=8$, $\tau = 0.3$, and $S=2$.

V. Simulation Results

We consider a multi-cell VWN with $L=4$ RRHs connected to $B=3$ BBUs serving $K=8$ users in $S=2$ slices. The RRHs are located at coordinates: $(0.5,0.5),(0.5,1.5),(1.5,0.5)$ and $(1.5,1.5)$ in the 2×2 square area. The users are randomly allocated within this area, using uniform distribution. The channel power loss is modeled as $\beta_{l,k_s} = (d_{l,k_s})^{-\zeta}$ where $d_{l,k_s}>0$ is the distance between user k_s and the RRH l and $\zeta=3$ is the path loss exponent [27]. We assume each fronthaul link has a capacity of $c^{\max}_{l,b} = 5$ baseband signals. We set $P^{\max}_{k_s} = 0$ dB, $\forall k_s\in\mathcal{K}_s, \forall s\in\mathcal{S}$, $x_1 = 10^7$, $\varepsilon_1 = \varepsilon_3 = 10^{-5}$, $\varepsilon_2 = \varepsilon_4 = 10^{-6}$ and $M^{\max}_l = 150$, $\forall l$ unless otherwise stated. Also, $w_{k_s,b}, \forall k_s\in\mathcal{K}_s, \forall b\in\mathcal{B}$ is a random number between 1 and K. In all of the simulations, when there is no feasible solution for the system, i.e., any of the constraints given by (5) does not hold, the total rate is set to be zero.

In Fig. 2, the effect of minimum required rate of each SP on the total achieved rate of VWN is demonstrated. Here, we also compare the performance of the proposed algorithm with that of the traditional algorithm of wireless network in which each user is connected to the nearest RRH and the antennas of each RRH are divided fairly between the users connected to that RRH. All users send data with maximum power and each BBU selects the users with lowest $w_{k_s,b}$, to the maximum allowable number of supported users $O^{\max}_b$. As omit can be seen in Fig. 2, the total rate decreases with increasing R^{rsv}_s due to the reduction in the feasibility region for all approaches. Moreover, the total rate obtained in the case of perfect CSI is higher than that in the case of imperfect

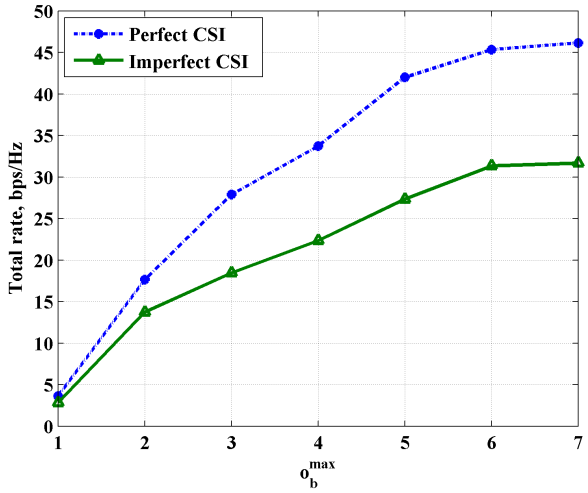

Fig. 3: Total rate versus $o_b^{\max}$ for $P_{k_s}^{\max} = 0$ dB,$M_l^{\max} = 150$, $L = 4$, $B = 3$ BBUs, $K = 12$, $\tau = 0.3$, and $S = 2$.

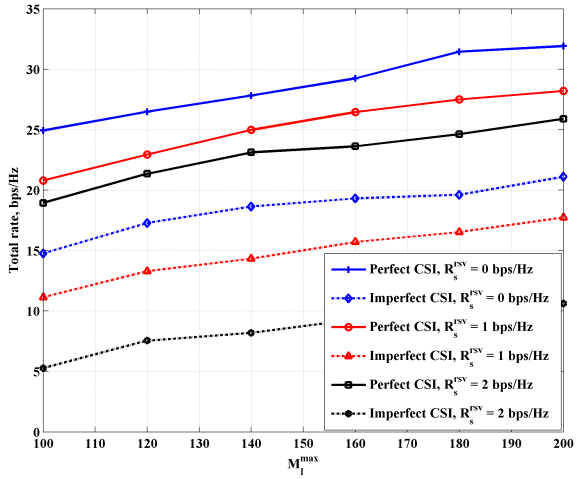

Fig. 4: Total rate versus $M_l^{\max}$ for $P_{k_s}^{\max} = 0$ dB, $L = 4$, $B = 3$ BBUs, $K = 8$, $o_b^{\max} = 3$, $\tau = 0.3$, $S = 2$.

CSI due to the interference from pilot contamination from users in neighboring RRHs. Also, from Fig. 2, the proposed algorithm outperforms the traditional approach for both perfect and imperfect CSI scenarios, which highlights the benefits of centralized resource management in C-RAN to increase the performance of VWN by setting parameters of network in the central BBU.

Fig. 3 shows the effect of capability of signal processing of each BBU, i.e., o_b^{max}, on the total rate of VWN. As observed, the total rate obtained with perfect CSI estimation is always higher than that with the imperfect CSI scenario, which implies the importance of CSI estimation in the massive-MIMO aided C-RAN. Moreover, the total rate increases with $o_b^{\max}$. Note that, by increasing the o_b^{max}more than 6, the rate is not increased significantly. Thus, having $o_b^{\max} > 6$ is not more beneficial.

The benefits of massive MIMO are shown in Fig. 4 by considering different numbers of antennas. This figure indicates that the total rate increases with increasing $M_l^{\max}$ due to the spatial multiplexing gain obtained from the increase in the number of antennas. Again, the total rate with perfect CSI is higher that with imperfect CSI, and the total rate decreases with increasing R_s^{rsv}, similar to Fig. 2.

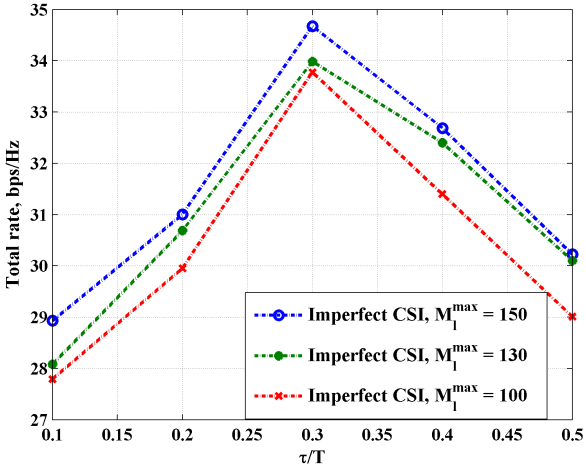

Fig. 5: Total rate versus τ/T for different $M_l^{\max}$ for $P_{k_s}^{\max} = 0$ dB, $L = 4$, $B = 3$, $K = 8$, $o_b^{\max} = 3$, and $S = 2$.

To get more insight about the effect of pilot duration, in Fig. 5, the total rate versus τ/T is shown. From Fig. 5, the total rate keeps increasing as τ/T increases up to $\tau/T = 0.3$ and then decreases. This is because at very low values of τ, the pilot contamination effect is more pronounced. However, as τ keeps increasing, there is less data transmission time and more time is allocated to send pilot transmission. Hence, a proper design of the pilot duration is essential in order to maintain high efficiency of the VWN and based on the simulation results, $\tau/T = 0.3$ is optimal for this setup. Fig. 5 also demonstrates the tradeoff between CSI accuracy and the VWN performance.

VI. Conclusion

In this paper, we presented a study on the resource allocation problem for VWN in a fronthaul-limited C-RAN. Specifically, we considered a multi-cell VWN supporting different slices with the user to RRH/BBU allocation constraints. We proposed a two-step iterative algorithm that jointly associates users to RRHs and BBUs, and allocates power and antennas with the aim of maximizing the system sum rate, while maintaining the slice isolation. Via simulation results, the performance of the proposed algorithm is evaluated for both imperfect and perfect CSI estimation scenarios. The effects of the fronthaul limitation and pilot contamination error on the system performance are investigated.

Appendix

A. Proof of achieved rates in perfect and imperfect CSI scenarios

1) For perfect CSI case, the up-link received signal from user $k_s \in \mathcal{K}_s$ on sub-carrier n at RRH l is [27]

$$r_{l,k_s}(\text{Perf.}) = \sqrt{p_{l,k_s}}\mathbf{a}_{l,k_s}\mathbf{h}_{l,k_s}x_{l,k_s} + \mathbf{a}_{l,k_s}\boldsymbol{\sigma}_{l,k_s} + \qquad (21)$$

$$\sum\nolimits_{l'\in\mathcal{L},l'\neq l}\sum\nolimits_{s\in S}\sqrt{p_{l',k_s}}\mathbf{a}_{l',k_s}\mathbf{h}_{l',k_s}x_{l',k_s},$$

where $\mathbf{h}_{l,k_s}$ is the vector of all $h_{l,k_s,m}$ for all $m\in\mathcal{M}$, x_{l,k_s} is the transmit symbol, $\mathbf{a}_{l,k_s}\in\mathbb{C}^{1\times M_{l,k_s}}$ is the linear detector vector, and $\boldsymbol{\sigma}_{l,k_s}$ is the corresponding noise coefficient vector. For maximum ratio combing (MRC) detector, we have $\mathbf{a}_{l,k_s}=\mathbf{h}_{l,k_s}^{\dagger}$, where † denotes the conjugate transpose operation. Thus, the received signal vector is [27]

$$r_{l,k_s}(\text{Perf.})=\sqrt{p_{l,k_s}}(\mathbf{h}_{l,k_s})^{\dagger}\mathbf{h}_{l,k_s}x_{l,k_s}+\mathbf{h}_{[l,k_s]^{\dagger}}\mathbf{n}_{[l,k_s]}+\sum\nolimits_{\forall l'\in\mathcal{L},l'\neq l}\sum\nolimits_{\forall s\in S}\sqrt{p_{l',k_s}}(\mathbf{h}_{l,k_s})^{\dagger}\mathbf{h}_{l',k_s}x_{l',k_s} \quad (22)$$

If $M_{l,k_s}\gg 1$, from the law of large numbers, $\sum_{\forall l'\in\mathcal{L},l'\neq l}\sum_{\forall s\in S}\sqrt{p_{l',k_s}}(\mathbf{h}_{l,k_s})^{\dagger}\mathbf{h}_{l',k_s}x_{l',k_s}$ in (22) becomes zero [27]. Considering $p^{[k_s l]}=E_{l,k_s}/M_{l,k_s}$, (22) is

$$\frac{1}{\sqrt{M_{l,k_s}}}r_{l,k_s}=\sqrt{E}_{l,k_s}\beta_{l,k_s}x_{l,k_s}+\sqrt{\beta}_{l,k_s}\tilde{n}_{l,k_s}, \quad (23)$$

where $\tilde{n}_{l,k_s}$ represents the AWGN with power 1. Hence, the SINR from user k_s in slice s and RRH l converges to (2).

2) For imperfect CSI, $\boldsymbol{\Phi}$ represents the $\tau\times K$ orthonormal pilot sequence matrix where $\boldsymbol{\Phi}^H\boldsymbol{\Phi}=\mathbf{I}_K$ and $\mathbf{I}_K$ is the unit matrix. In this case, the estimated CSI is [27]

$$\tilde{h}_{l,k_s,m}=\left(h_{l,k_s,m}+\frac{1}{\sqrt{p_{l,k_s}(\text{Pilot})}}w_l\right)\tilde{\beta}_{l,k_s},$$

where $\tilde{\beta}_{l,k_s}=\beta_{l,k_s}(\sum_{l\in\mathcal{L}}\sum_{k_s\in\mathcal{K}_s}\sum_{s\in\mathcal{S}}\beta_{l,k_s}+\frac{1}{p_{l,k_s}(\text{Pilot})})^{-1}$ and $p_{l,k_s}(\text{Pilot})$ is the transmit power for the pilot sequence for the user k_s and w_l represents the contaminated pilot sequence received at the RRH l. Now, the received signal after using MRC at the RRH l from user k_s is

$$r_{l,k_s}(\text{Imperf.})=\tilde{\mathbf{h}}_{l,k_s}^{\dagger}(\sqrt{p_{l,k_s}}\mathbf{h}_{l,k_s}x_{l,k_s}+\mathbf{n}_{l,k_s}+\sum_{\forall l'\in\mathcal{L},l'\neq l}\sum_{\forall s\in S}\sum_{\forall k_s'\in\mathcal{K}_s,k_s'\neq k_s}\sqrt{p_{l',k_s'}}\mathbf{h}_{l',k_s'}x_{l',k_s'})$$

Considering $p_{l,k_s}=E_{l,k_s}/\sqrt{M}_{l,k_s}$ and $p_{p,l,k_s}=\tau p_{l,k_s}$ in the above expression, and by using the law of large numbers for large M_{l,k_s}, the SINR of the user k_s is (3) [27].

B. Proof of Proposition 1

The objective function in (5) can be expressed as:

$$\min_{\boldsymbol{\alpha},\mathbf{F}}-\sum_{s\in\mathcal{S}}\sum\nolimits_{\forall l\in\mathcal{L}}\sum\nolimits_{\forall k_s\in\mathcal{K}_s}F_{k_s}(t_1)\alpha_{l,k_s}(t_1)R_{l,k_s}(t) \quad (24)$$

To ensure the objective function of GP is positive, we apply

$$x_1-\sum\nolimits_{\forall s\in\mathcal{S}}\sum\nolimits_{\forall l\in\mathcal{L}}\sum\nolimits_{\forall k_s\in\mathcal{K}_s}F_{k_s}(t_1)\alpha_{l,k_s}(t_1)R_{l,k_s}(t)$$

where $x_1\gg 1$. By considering t_1, we use $x_0(t_1)>0$ to transform the above expression into

$$\min_{\boldsymbol{\alpha}(t_1),\mathbf{F}(t_1),x_0(t_1)}\ x_0(t_1) \quad (25)$$

$$x_1-\sum_{\forall s}\sum_{\forall l}\sum_{\forall k_s}F_{k_s}(t_1)\alpha_{l,k_s}(t_1)R_{l,k_s}(t)\leq x_0(t_1). \quad (26)$$

Now, (26) can be rewritten as

$$\frac{x_1}{x_0(t_1)+\sum_s\sum_{\forall l}\sum_{\forall k_s}F_{k_s}(t_1)\alpha_{l,k_s}(t_1)R_{l,k_s}(t)}\leq 1,$$

and by using AGMA, we get

$$x_1\big[\frac{x_0(t_1)}{c_0(t_1)}\big]^{-c_0(t_1)}\prod_{\forall l,k_s}\big[\frac{F_{k_s}(t_1)\alpha_{l,k_s}(t_1)R_{l,k_s}(t)}{c_{l,k_s}(t_1)}\big]^{-c_{l,k_s}(t_1)}\leq 1,$$

where, $c_0(t_1)$ and $c_{l,k_s}(t_1)$ are defined in (8) and (9). Similarly, C6 can be expressed as

$$\frac{R_s^{\text{rsv}}}{\sum_{\forall l\in\mathcal{L}}\sum_{\forall k_s\in\mathcal{K}_s}F_{k_s}(t_1)\alpha_{l,k_s}(t_1)R_{l,k_s}(t)}\leq 1,\quad\forall s\in\mathcal{S},$$

which can be approximated as

$$\widetilde{\text{C6}}: R_s^{\text{rsv}}\prod_{l,k_s}\big[\frac{F_{k_s}(t_1)\alpha_{l,k_s}(t_1)R_{l,k_s}(t)}{\varphi_{l,k_s}(t_1)}\big]^{-\varphi_{l,k_s}(t_1)}\leq 1, \quad (27)$$

where $\varphi_{l,k_s}(t_1)$ is defined in (11). Similarly, by applying AGMA to obtain the monomial approximation for C2 and C4, we obtain $\widetilde{\text{C2}}$ and $\widetilde{\text{C4}}$ with the approximation coefficients defined in (8)-(12). Therefore, (7) is derived.

C. Proof of Proposition 2

For the perfect scenario, the objective function of (13) is

$$\min_{\mathbf{P},\mathbf{M}}\prod\nolimits_{\forall l,k_s,s}\left(\frac{1}{1+\beta_{l,k_s}P_{l,k_s}M_{l,k_s}}\right),$$

the denominator of which can be expressed as

$$\omega_{l,k_s}(t_2)^{-\omega_{l,k_s}(t_2)}\big[(\beta_{l,k_s}P_{l,k_s}(t_2)M_{l,k_s}(t_2))/j_{l,k_s}(t_2)\big]^{j_{l,k_s}(t_2)},$$

where, ω_{l,k_s} and $j_{l,k_s}(t_2)$ are defined in (15). Now, the objective function can be written as

$$\min_{\mathbf{P},\mathbf{M}}\prod\nolimits_{\forall l,k_s,s}\Big[\omega_{l,k_s}(t_2)^{\omega_{l,k_s}(t_2)}\times\big[(\beta_{l,k_s}P_{l,k_s}(t_2)M_{l,k_s}(t_2))/j_{l,k_s}(t_2)\big]^{-j_{l,k_s}(t_2)}\Big]. \quad (28)$$

Consequently, C6 and C7 can be approximated as $\overline{\text{C6}}$ and $\overline{\text{C7}}$ as shown in (14). Hence, the overall problem for perfect CSI of sub-algorithm 2 is written as (14). where $\omega_{l,k_s}(t_2)$, $j_{l,k_s}(t_2)$, and $\lambda_{l,k_s}(t_2)$ are derived from (15), (16) and (17).

For the imperfect CSI scenario, the rate of user k_s in imperfect CSI scenario can be rewritten as

$$R_{l,k_s}=\log_2\left(\frac{1+\tau\sum_{\forall l}\sum_{\forall k_s}\sum_{\forall s}\beta_{l,k_s}^2P_{l,k_s}^2M_{l,k_s}}{1+\tau\sum_{\forall l'\neq l}\sum_{\forall k_s'\neq k_s}\sum_{\forall s}\beta_{l',k_s'}^2P_{l',k_s'}^2M_{l',k_s'}}\right). \quad (29)$$

Hence, the objective function of (13) can be rewritten as

$$\min_{\mathbf{P},\mathbf{M}}\prod_{l,k_s,s}\left(\frac{1+\tau\sum_{\forall l'\neq l}\sum_{\forall k_s'\neq k_s}\sum_{\forall s}\beta_{l',k_s'}^2P_{l',k_s'}^2M_{l',k_s'}}{1+\tau\sum_{\forall l}\sum_{\forall k_s}\sum_{\forall s}\beta_{l,k_s}^2P_{l,k_s}^2M_{l,k_s}}\right),$$

Now, by considering t_2 as the iteration index, the denominator of the above can be transformed by AGMA as

$$g_1(t_2)^{-g_1(t_2)}\prod_{l,k_s,s}\big[(\tau\beta_{l,k_s}^2P_{l,k_s}^2(t_2)M_{l,k_s}(t_2))g_{l,k_s}(t_2)\big]^{-g_{l,k_s}(t_2)}$$

where $g_1(t_2)$ and $g_{l,k_s}(t_2)$ are introduced in (19) and (20). Consequently, (13) is approximated to its GP format in (18).

REFERENCES

[1] J. G. Andrews, S. Buzzi, W. Choi, S. V. Hanly, A. Lozano, A. C. K. Soong, and J. C. Zhang, "What will 5G be?" *IEEE Journal on Selected Areas in Communications*, vol. 32, no. 6, pp. 1065–1082, June 2014.

[2] B. Cao, F. He, Y. Li, C. Wang, and W. Lang, "Software defined virtual wireless network: framework and challenges," *IEEE Network*, vol. 29, no. 4, pp. 6–12, July 2015.

[3] M. Peng, Y. Sun, X. Li, Z. Mao, and C. Wang, "Recent advances in cloud radio access networks: System architectures, key techniques, and open issues," *IEEE Communications Surveys Tutorials*, vol. 18, no. 3, pp. 2282–2308, third-quarter 2016.

[4] C. Liang and F. R. Yu, "Wireless network virtualization: a survey, some research issues and challenges," *IEEE Communciations Surveys and Tutorials*, vol. 17, no. 1, pp. 350–380, August 2014.

[5] S. Parsaeefard, V. Jumba, M. Derakhshani, and T. Le-Ngoc, "Joint resource provisioning and admission control in wireless virtualized networks," in *IEEE Wireless Commun. Netw. Conf. (WCNC)*, Mar. 2015, pp. 2020–2025.

[6] "C-RAN: The road towards green RAN," in *White Paper*. China Mobile, 2013.

[7] R. Wang, H. Hu, and X. Yang, "Potentials and challenges of C-RAN supporting multi-RATs toward 5G mobile networks," *IEEE Access*, vol. 2, pp. 1187–1195, 2014.

[8] M. Peng, C. Wang, V. Lau, and H. V. Poor, "Fronthaul-constrained cloud radio access networks: insights and challenges," *IEEE Trans. Wireless Commun.*, vol. 22, no. 2, pp. 152–160, 2015.

[9] "Suggestions on potential solutions to C-RAN," in *NGMN Alliance*, Jan. 2013.

[10] H. Q. Ngo, M. Matthaiou, and E. G. Larsson, "Massive MIMO with optimal power and training duration allocation," vol. 3, pp. 605 – 608, 2014.

[11] Z. Q. Luo and S. Zhang, "Dynamic spectrum management: Complexity and duality," *IEEE Journal of Selected Topics in Signal Processing*, vol. 2, no. 1, pp. 57–73, February 2008.

[12] G. Xu, "Global optimization of signomial geometric programming problems," *European Journal of Operational Research*, vol. 233, no. 3, pp. 500–510, 2014.

[13] S. Parsaeefard, R. Dawadi, M. Derakhshani, and T. Le-Ngoc, "Joint user-association and resource-allocation in virtualized wireless networks," *IEEE Access*, vol. 4, pp. 2738–2750, June 2016.

[14] M. Grant and S. Boyd, "CVX: Matlab software for disciplined convex programming, version 2.1," http://cvxr.com/cvx, 2014.

[15] A. Liu and V. K. N. Lau, "Joint power and antenna selection optimization in large cloud radio access networks," *IEEE Transactions on Signal Processing*, vol. 62, no. 5, p. 13191328, 2014.

[16] R. Z. Shixin Luo and T. J. Lim, "Downlink and uplink energy minimization through user association and beamforming in c-ran," *IEEE Transactions on Wireless Communications*, vol. 14, no. 1, pp. 494–508, 2015.

[17] C. Liang, and F. R. Yu, "Distributed resource allocation in virtualized wireless cellular networks based on ADMM," in *IEEE Intl. Conf. on Computer Commun. (INFOCOM)*, April 2015, pp. 360–365.

[18] H. Ahmadi, I. Macaluso, I. Gomez, L. Doyle, and L. A. DaSilva, "Substitutability of spectrum and cloud-based antennas in virtualized wireless networks," *IEEE Wireless Communications*, vol. PP, no. 99, pp. 2–8, Dec. 2016.

[19] T. Leanh, N. H. Tran, D. T. Ngo, and C. S. Hong, "Resource allocation for virtualized wireless networks with backhaul constraints," *IEEE Communications Letters*, vol. 21, no. 1, pp. 148 – 151, Oct. 2016.

[20] B. Cao, W. Lang, Y. Li, Z. Chen, and H. Wang, "Power allocation in wireless network virtualization with buyer/seller and auction game," in *IEEE Global Commun. Conf. (GLOBECOM)*, Feb. 2015, pp. 1–6.

[21] H. Ibrahim, H. ElSawy, U. T. Nguyen, and M. Alouini, "Modeling virtualized downlink cellular networks with ultra-dense small cells," in *IEEE Intl. Conf. Commun. (ICC)*, June 2015, pp. 5360–5366.

[22] H. Zhang, W. Wang, X. Li, and H. Ji, "User association scheme in Cloud-RAN based small cell network with wireless virtualization," in *IEEE Intl. Conf. on Computer Commun. (INFOCOM)*, May 2015, pp. 384–389.

[23] Z. Chang, Z. Han, and T. Ristaniemi, "Energy efficient optimization for wireless virtualized small cell networks with large scale multiple antenna," *IEEE Communications Transactions*, vol. PP, no. 99, pp. 1–12, Feb. 2017.

[24] V. N. Ha, L. B. Le, and N. D. Dao, "Cooperative transmission in Cloud RAN considering fronthaul capacity and cloud processing constraints," in *IEEE Wireless Commun. Netw. Conf. (WCNC)*, Apr. 2014, pp. 1862–1867.

[25] A. Checko, H. Christiansen, Y. Yan, L. Scolari, G. Kardaras, M. Berger, and L. Dittmann, "Cloud RAN for mobile networks- A technology overview," *IEEE Commun. Surveys Tuts.*, vol. 17, no. 1, pp. 405–426, First quarter 2015.

[26] L. Lu, G. Li, A. Swindlehurst, A. Ashikhmin, and R. Zhang, "An overview of massive MIMO: Benefits and challenges," *IEEE J. Sel. Topics Signal Process.*, vol. 8, pp. 742–758, Oct. 2014.

[27] H. Q. Ngo, E. G. Larsson, and T. L. Marzetta, "Energy and spectral efficiency of very large multiuser MIMO systems," *IEEE Trans. Commun.*, vol. 61, no. 4, pp. 1436–1449, 2013.

[28] R. Kokku, R. Mahindra, H. Zhang, and S. Rangarajan, "NVS: A substrate for virtualizing wireless resources in cellular networks," *IEEE/ACM Trans. Netw.*, vol. 20, no. 5, pp. 1333–1346, Oct. 2012.

[29] S. Boyd and L. Vandenberghe, *Convex Optimization*. Cambridge University Press, 2009.

[30] M. Razaviyayn, M. Hong, and Z. Q. Lue, "A unified convergence analysis of block successive minimization methods for nonsmooth optimization," *SIAM Journal on Optimization*, vol. 23, no. 2, pp. 1126–1153, 2013.

Saeedeh Parsaeefard (S09M14) received the B.Sc. and M.Sc. degrees from Amirkabir University of Technology (Tehran Polytechnic), Tehran, Iran, in 2003 and 2006, respectively, and the Ph.D. degree in electrical and computer engineering from Tarbiat Modares University, Tehran, in 2012. She was a Post-Doctoral Research Fellow with the Telecommunication and Signal Processing Laboratory in the Department of Electrical and Computer Engineering at the McGill University, Canada from October 2013 to September 2013. From November 2010 to October 2011, she was a Visiting Ph.D. Student with the Department of Electrical Engineering, University of California, Los Angeles, CA, USA. Her current research interests include the applications of robust optimization theory and game theory on the resource allocation and management in wireless networks.

Rajesh Dawadi received the B.Tech. degree in Electronics and Communication engineering from Maulana Azad National Institute of Technology (MANIT), Bhopal, India in 2012 and is currently pursuing his M.Eng degree in Electrical engineering from McGill University, Montreal, QC, Canada under the supervision of Professor Tho Le-Ngoc. From 2012-2014, he was with Reliance Jio InfoComm Limited, Mumbai, India where he worked on the TD-LTE eNodeB development and validation. His research interests include dynamic resource allocation and energy efficiency in wireless networks.

Mahsa Derakhshani (S10-M13) received the B.Sc. and M.Sc. degrees from Sharif University of Technology, Tehran, Iran, in 2006 and 2008, respectively, and the Ph.D. degree from McGill University, Montreal, QC, Canada, in 2013, all in electrical engineering. From 2013 to 2015, she was a Postdoctoral Research Fellow with the Department of Electrical and Computer Engineering, University of Toronto, Toronto, ON, Canada, and a Research Assistant with the Department of Electrical and Computer Engineering, McGill University. From 2015 to 2016, she was an Honorary NSERC Postdoctoral Fellow with Department of Electrical and Electronic Engineering, Imperial College London. She is currently a Lecturer in Digital Communications with the Wolfson School of Mechanical, Electrical and Manufacturing Engineering, Loughborough University. Her research interests include radio resource management for wireless networks, software-defined wireless networking, applications of convex optimization and game theory for communication systems, and spectrum sensing techniques in cognitive radio networks. Dr. Derakhshani received the John Bonsall Porter Prize, the McGill Engineering Doctoral Award, the Fonds de Recherche du QuebecNature et Technologies (FRQNT) and Natural Sciences and Engineering Research Council of Canada (NSERC) Postdoctoral Fellowships.

THO LE-NGOC received the B.Eng. (Hons.) in electrical engineering and the M.Eng. from McGill University, Montreal, Canada, in 1976 and 1978, respectively, and the Ph.D. degree in digital communications from the University of Ottawa, Canada, in 1983. From 1977 to 1982, was a R&D Senior Engineer with Spar Aerospace Ltd., Sainte-Anne-de-Bellevue, Canada, and involved in the development and design of satellite communications systems. From 1982 to 1985, he was the Engineering Manager of the Radio Group with the Department of Development Engineering of SRTelecom Inc., St.Laurent, Canada, where he developed the new point-to-multipoint DA-TDMA/TDM Subscriber Radio System SR500. From 1985 to 2000, he was a Professor with the Department of Electrical and Computer Engineering, Concordia University, Montreal. Since 2000, he has been with the Department of Electrical and Computer Engineering, McGill University. His research interest is in the area of broadband digital communications. He is a fellow of the Engineering Institute of Canada, the Canadian Academy of Engineering, and the Royal Society of Canada. He is the recipient of the 2004 Canadian Award in Telecommunications Research, and the IEEE Canada Fessenden Award 2005. He holds a Canada Research Chair (Tier I) on Broadband Access Communications.

Mina Baghani received the B.Sc. and M.Sc. degrees from Shahed University, Tehran, Iran, in 2008 and 2011, respectively and the Ph.D. degree in electrical engineering from Amirkabir University of Technology (Tehran Polytechnic), Tehran, Iran, in 2017 . Her current research interests include multilayer coding, nonlinear optimization methods, cognitive radio networks, and resource allocation in wireless networks.